TITLE: Plastic Envelope in Propagating Crack Wake on Al-Li Alloys Subjected to Fatigue Cycles and to Different Heat Treatments

TITLE: New Metallic Materials for the Structure of Aging Aircraft [les Nouveaux Materiaux metalliques pour les structures des aeronefs d'ancienne generation]

Plastic envelope in propagating crack wake on Al-Li alloys subjected to fatigue cycles and to different heat treatments

S. Corradi,* M. Marchetti† and W. Stellino‡
School of Aerospace Engineering
University of Rome "La Sapienza"
Via Eudossiana 16, 00184 Rome, Italy

Summary. The aim of this research is to study the fracture behaviour of three Al-Li alloys (2091-2195-8090), using standard CT specimens, in the frequency range of 1-10 Hz. Each of these three alloys is subjected to different heat treatments and its homogeneity is analysed, before and after treatments, by Scanning Electron Microscope (SEM). Crack tip opening displacements and plastic zone envelope analyses are fully treated by experimental and numerical results and fatigue crack growth process is extensively reported. At the end of fatigue tests, specimen fracture surfaces have been deeply analysed by SEM in order to individualise the characteristics of fracture as function of frequency, ΔK and load ratio R.

Key words: crack growth, plasticity, CT specimen, SEM.

1. INTRODUCTION

Renewed and extensive research and development activities led to new generation of Al-Li alloys by three major producers: Alcon, Alcoa and Pechiney. For these alloys the improvements in various properties, including density and stiffness, result from lithium additions and have the potential to save up to 10% in weight by direct substitution, and up to 18% in weight if the increased specific stiffness (modulus/density) is performed [1] [2].

Commercial aluminium-lithium alloys are targeted as advanced materials for aerospace technology primarily because of their low density, high specific modulus, and excellent fatigue and cryogenic toughness properties. The superior fatigue crack propagation resistance of Al-Li alloys, in comparison with other traditional alloys, is primarily due to high levels of crack tip shielding, meandering crack paths and resultant roughness-induced crack closure.

However, the fact that these alloys derive their superior properties extrinsically from the above mechanisms has certain implications with respect to small crack and variable amplitude behaviour. For example, aluminium-lithium alloys loose their fatigue advantage over conventional aluminium alloys in compression dominated variable amplitude fatigue spectra tests. However, in tension dominated spectra, aluminium-lithium alloys show greater retardation on the application of single peak tensile overloads. The principal disadvantages of peak strength aluminium-lithium alloys are reduced ductility and fracture toughness in the short transverse direction, anisotropy of in plane properties and accelerated fatigue crack extension rates when cracks are microstructurally small. These limitations have imposed the direct substitution of aluminium airframe alloys with aluminium-lithium alloys, although it is possible to group the present aluminium alloys and the current aluminium-lithium alloys in terms of product form and of primary design criteria.

During the past 20 to 30 years influences on crack growth behaviour have been systematically investigated. It was found that the mean stress applied is important and its effect is closely correlated to crack closure behaviour. In recent years the threshold behaviour had also been extensively investigated. Doker [3] showed that most of the da/dN vs. ΔK data for different materials which are presently available fall below some limiting curves. The experimental data show that they fall comparatively close together for different R ratios in the middle part of the curve (mean stress). At the lower and higher ends of the curve, data for different material considerably deviate according respectively to crack closure effect and to fracture toughness K_c values.

The aim of this research is to investigate, by means of experimental and numerical analyses, fatigue behaviour of 2091, 8090 and 2195 aluminium-lithium alloys and it has mainly two purposes: 1) to define frequency effects on crack propagation rate and 2) to survey plastic zone

* Research Scientist
† Full Professor
‡ Graduate Student

Paper presented at the RTO AVT Workshop on "New Metallic Materials for the Structure of Aging Aircraft", held in Corfu, Greece, 19-20 April 1999, and published in RTO MP-25.

progress, as function of time and space, over crack tip. First purpose was carried out by experimental tests. These were all performed in the same operating conditions: that is, same environment (lab air), same loads, same specimens geometry whereas the only variable parameter was the frequency. Testing frequency range has been 1-10 Hz.
The second part required use of an elasto-plastic analytical model, which has actual crack length (experimental data) as input and gives out, as output, the plastic zone size together with length, width and abscissa of all elements (totally ten) used to describe it. A comparison will be carried out 1) among different alloys, for the same testing conditions, and 2) for the same alloy, for different frequency values. The research is concluded with presentation of fracture surface analysis by SEM.

2. THE PROPOSED APPROACH

A two dimensional, weight function based, non linear elasto-plastic analytical model has been used for considering plastic zone evolution. This model is restricted to two dimensional cracked bodies with cracks under mode I loading. Using predictions of crack opening stress, the effective stress intensity factor range, at fatigue crack tip under a given cyclic loading, is computed. The effect of residual stress on fatigue crack propagation is of great practical significance and has been the focus of much research. Superposition techniques are often used when assessing the effects of fatigue crack propagation. The superposition involves the computation of the stress intensity factor, which is associated with the initial pre-existing *residual* stress field. This factor is then superposed upon the stress intensity factor that results from *external* loading, to give the total stress intensity factor as:

$$K = K_{res} + K_{ext} \qquad (1)$$

Maximum and minimum values of the total resultant stress intensity factor K are computed for the cyclic loading and a total resultant stress intensity factor range ΔK is calculated. This resultant stress intensity factor range may then be used to compute the predicted fatigue crack growth rate da/dN using a $da/dN=f(\Delta K)$ correlation.
The superposition technique is used extensively because of its simplicity. It has been criticised by some researchers because it considers only the initial residual stress field that exists in the uncracked structure, with no acknowledgement of the redistribution of residual stress that occurs as the propagating fatigue crack penetrates, with its free or partially free surfaces, the residual stress field. Other researchers have argued that the redistribution of residual stress is of no consequence.
Bueckner (1958) has demonstrated mathematically that, for linear elastic materials, stress intensity factors resulting from a given applied loading may be computed using the stress distribution in the uncracked structure. Heaton [4] has presented a mathematically rigorous proof that generalises Bueckner's formulation to include both thermal and residual stress fields. These works suggest that, for linear elastic materials, the redistribution of applied and residual stresses due to fatigue crack propagation is of no consequence when computing stress intensity factors and fatigue crack growth through use of correlation $da/dN=f(\Delta K)$.
These conclusions are applicable to linear elastic materials only. The existence of plastic deformation at the crack tip, even under small scale yielding conditions, will produce crack generated residual stresses at the crack tip and crack closure along the crack surfaces of a propagating crack. The superposition methodology is unable to account for the influence of these non linear plasticity effects. Consequently, the use of linear elastic superposition techniques for prediction of the effects of residual stress on fatigue crack propagation and plastic zone evolution, may result in predictions that correlate poorly with experimental observations. More accurate predictions may be possible if an increased understanding is established of the interactions between residual stress fields and crack closure.
The model used here is an extension of Newman's Model [5]. While Newman investigated specific two dimensional geometry, the model described here accommodates the analysis of any two dimensional geometry that exhibits a crack emanating from a free surface for which a weight function is known.
Let's consider a propagating fatigue crack being closed by plastic deformation at crack tip and propped open by a wake of plastically deformed material along the crack surfaces. A series of rigid perfectly plastic elements is used to model the residual plastic deformation along the fatigue

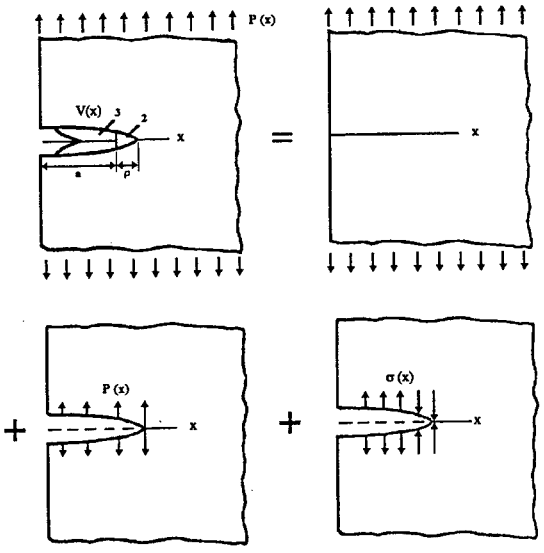

Figure 1: Elasto-plastic fatigue crack model as superposition of elastic ones

crack surfaces and the plastic zone ahead of the propagating crack. The model is constructed using a superposition of two elastic crack problems and is based on the Dugdale Model, modified to leave plastically deformed material along the crack surfaces as the crack advances.
The external loading is assumed to vary between a fixed maximum value S_{max} and a fixed minimum S_{min}; thus only constant amplitude applied loading is considered. Stress $\sigma(x)$ is generated along crack surfaces as a consequence of plastic deformation at the crack tip and of residual plastic deformation along the crack surfaces. The model is composed of three region as indicated in Fig. 1.

1. A linear elastic region containing a fictitious crack of length $d = a + \rho$;
2. A plastic region of length ρ ahead of the actual crack
3. A region of residual plastic deformation along the crack surfaces

The plastic and residual plastic deformation regions have been modelled using n rigid perfectly plastic bar elements as shown in Fig. 2. To approximate the effects of strain hardening, the flow stress σ_0 is taken to be the average value between the yield and the ultimate strength. The generic stress σ_j is applied on the linear elastic region and is transmitted to this region by the n bar elements as illustrated in Fig. 2.

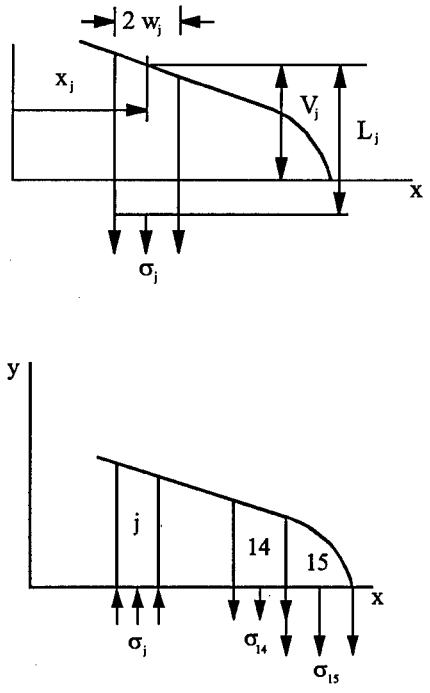

Figure 2: Elements and applied stresses

As originally postulated by Dugdale, under a tensile stress $\sigma(x)$, element 15 would yield in tension and crack opening would be restrained.
Generic element j is located along and attached to the upper crack surface. Under low levels of $\sigma(x)$, crack remain closed at j, placing element j in compression, and thus propping open the crack as shown. Under higher levels of $\sigma(x)$ the crack would open and $\sigma_j \rightarrow 0$. The plastic zone ahead of the current crack tip under the maximum applied loading is modelled using ten elements. The plastic zone size is computed assuming finite stresses at the fictitious crack tip as originally postulated by Dugdale. Element widths w are assumed such that elements near the actual crack tip are smaller in width, while element lengths L, in the plastic zone, are given by weight function based computation. An initial edge crack length a is assumed to exist and it is modelled using elements 1-5, with element 1 located at the crack mouth. These elements have negligible length.
Weight function $m(x, a)$, which remains valid for $a/W < 0.5$ [6], and crack tip opening displacement $V(x_i)$ expressions are as follows:

$$m(x,a) = \frac{1}{\sqrt{2\pi(a-x)}}\left[1 + m_1\left(1 - \frac{x}{a}\right) +\right.$$

$$+ \; m_2\left(1-\frac{x}{a}\right)^2\Bigg]$$

$$V(x_i) = \frac{2}{E'}\int_{x_i}^{d} m(x_i,\alpha)K_I(\alpha)d\alpha \qquad (2)$$

where m_1 and m_2 depend upon the ratio a/W between specimen width W and crack length a, α is a fictitious crack length, E' is the generalised Young modulus and K_I, which is the mode I stress intensity factor, is given by:

$$K_I(\alpha) = 2\int_0^{\alpha} T(x)m(x,\alpha)dx \qquad (3)$$

Combining and substituting the previous equations, the total generic displacement V_i results as

$$V_i = f(x_i, S_a) - \sum_{j=1}^{n}\sigma_j g(x_i, x_j) \qquad (4)$$

where the first term is the displacement due to external loading S when crack lenght is a and the second term represents the displacement in x_i due to the stress σ_j on the generic j element. The crack extension creates a new element with width w_i equal to Δa and length L_i equal to the crack tip opening displacement V_i before extension. In fact under maximum loading crack surfaces are completely opened and element lengths L_i result equal to surface displacements V_i. Under the minimum applied stress, elements representing the residual plastic deformation along the crack surfaces may come into contact and transmit a compressive stress; compressive yielding is also possible, requiring the computation of new element lengths. The stress along the line of crack propagation, that produces the first full opening of the crack, is defined as opening stress $\sigma_0 h(x)$, where σ_0 is a scaling parameter that defines the magnitude of the crack opening stress and $h(x)$ is a shape function which defines the crack opening stress along $y = 0$ (line of crack propagation). Under a uniform stress with no stress concentration, one obtains $h(x)$=1, while it varies if the geometry of interest exhibits a stress concentration.

Under constant amplitude loading, the last element to loose contact and open is generally the element along the crack surface closest to the crack tip. It is assumed that the only portion of the loading cycle that contributes to the crack propagation is the portion for which the crack is fully open, as originally postulated by Elber [7]. Small fatigue cracks induce limited plastic zones mostly providing plane strain conditions. As crack propagates and plastic zone size increases, a transition to plane stress condition can be observed. It results that crack growth analysis requires the modelling of both plane strain and plane stress conditions. In light of the introduction of a correction factor, which varies between 1 and 3, as demonstrated by Newman [5], the present model predicts accurately the crack propagation.

3. THE EXPERIMENTAL TESTS

The elasto-plastic model is used to survey plastic zone progress, as function of time and space, in a cyclically loaded edge cracked panel (CT specimen) as shown in Fig. 3. The constant amplitude loading was a uniform pulsating tension with R=0.3 and S_{max}=400 Kg. The panel width W is 40 mm. and an initial crack size a=6 mm. is assumed. The specimens used in the experimentation have been obtained in the LT configuration. The preparation of the surface has been particularly studied to facilitate the optical reading of the crack length; Knuth-Rotor System, that consists in using some rotating disks at constant speed on which are supported abrasive SiC papers, has been utilised. The cooling has been performed through a continuous throw of water, while the polish by some rotating cloths wetted by suspensions of allumina particles of 1 μm diameter. Finally, on both specimen faces some imprints, spaced 1 mm the one from the other, have been realised. The ultimate strength for the three alloys, in LT direction, are: 462 MPa for 2091 alloy, 557 MPa for 2195 alloy and 470 MPa for 8090 alloy.

Their section is reported in succession in Fig.4. Like other age-hardened aluminium alloys, aluminium-lithium alloys achieve precipitation strengthening by thermal ageing after a solution heat treatment. The age hardening of aluminium-lithium alloys involves the continous precipitation of δ' (Al_3Li) from a supersaturated solid solution. Aluminium-lithium based alloys are microstructurally unique. They differ from most of the aluminium alloys in that once the major strengthening precipitate (δ') is homogeneously precipitated, it remains coherent even after extensive ageing. All three alloys under examination have a temper designation of T8,

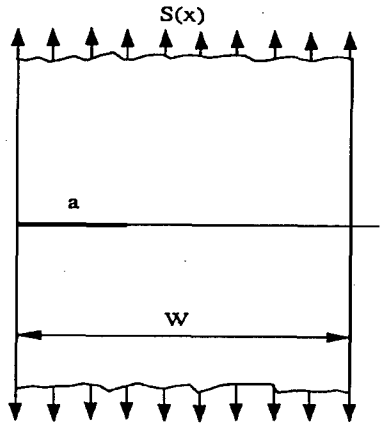

Figure 3: Finite width panel with edge crack a

which consists in a solution heat treatment, a cold working and an artificially ageing. Two of them, 8090 and 2091 alloy, have been subjected to a further treatment, designated as Tx51 (normally applied to plate and to rolled or cold finished rod and bar), which relieves residual stresses by stretching.
The measures of crack length have been performed by an optical microscope WILD M38, provided of an enlargement of 40X. Measures have been taken on both specimen sides and, periodically, each specimen has been removed and observed with the electron microscope or with an optical microscope that allows bigger enlargements.
Besides the necessary data for the determination of wake plastic strain, i.e. length, width and abscissa (as function of cycles number) of each of the ten elements, a parameter Ψ, which takes into consideration the crack opening and consequently keeps track of ΔK_{eff} and not simply of ΔK, is considered as,

$$\Psi = \frac{\Delta K_{eff}}{1 - S_0/S_{max}} \qquad (5)$$

Finally, the fracture surfaces have been observed by SEM (Scanning Electron Microscope). The same surfaces, attached subsequently by a specific acid solution (50 $ml\ H_2O$, 50 $ml\ HNO_3$, 32 $ml\ HCl$, 2 $ml\ HF$), have been studied with the scanning microscope for the individualisation of fracture plans and of flow directions.

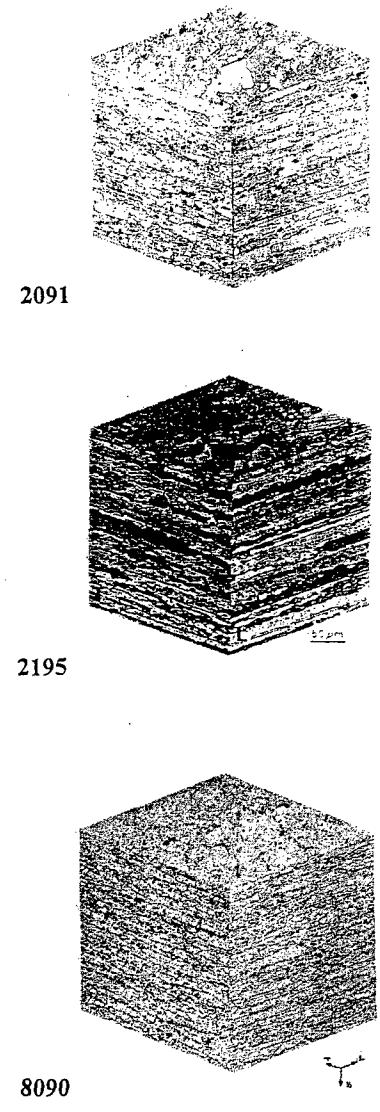

Figure 4: Section of the alloys under examination

4. RESULTS

The tests performed for the 8090 alloy are reported in Figg. 5-6. These allow to follow the crack evolution both in terms 1) of crack length vs the number of effected cycles and 2) of the evolution of plastic zone adimensional size ρ vs the number of cycles. From Fig. 5 is deduced, as confirmed by most bibliography, that, as frequency increases, the rate of propagation decreases and the ultimate number of cycles increases. Such conclusions are also confirmed by Fig. 6, where as frequency increases, the dimension of the plastic zone ρ (and therefore the degree of local plasticity present at the crack tip) tends to decrease. The tests performed for the 2195 alloy are reported in Figg. 7-8: same conclusions are valid both in terms of crack rate of propagation and in terms

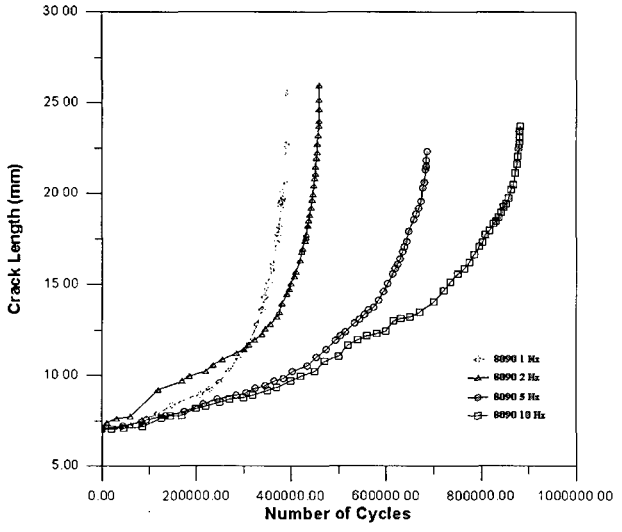

Figure 5: 8090 alloy

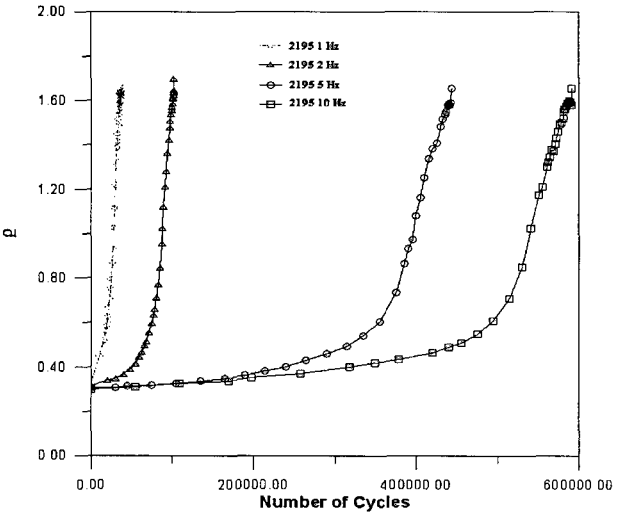

Figure 8: 2195 alloy

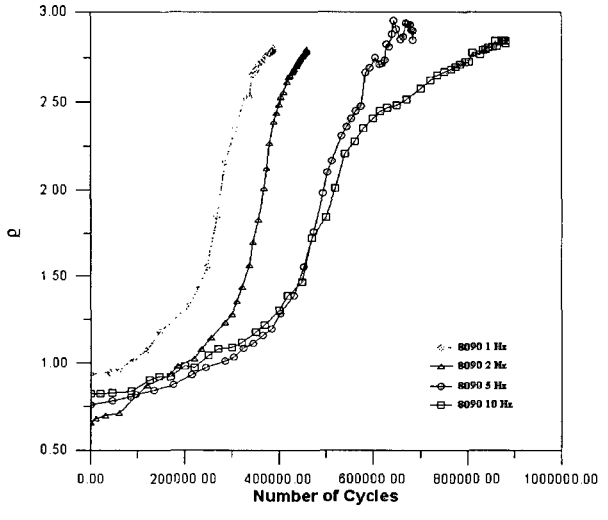

Figure 6: 8090 alloy

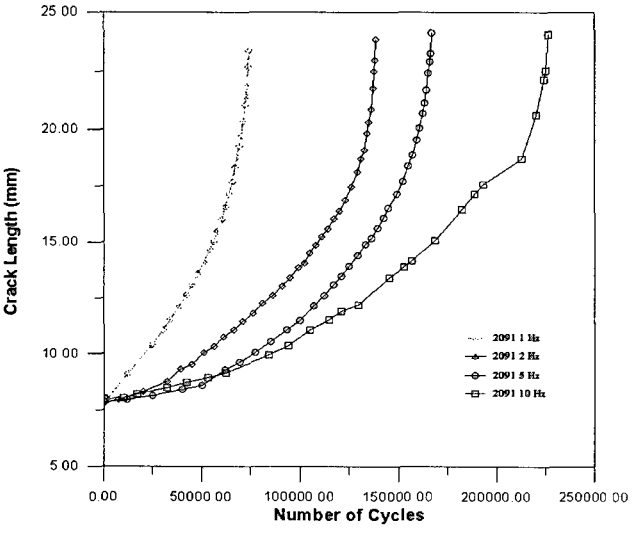

Figure 9: 2091 alloy

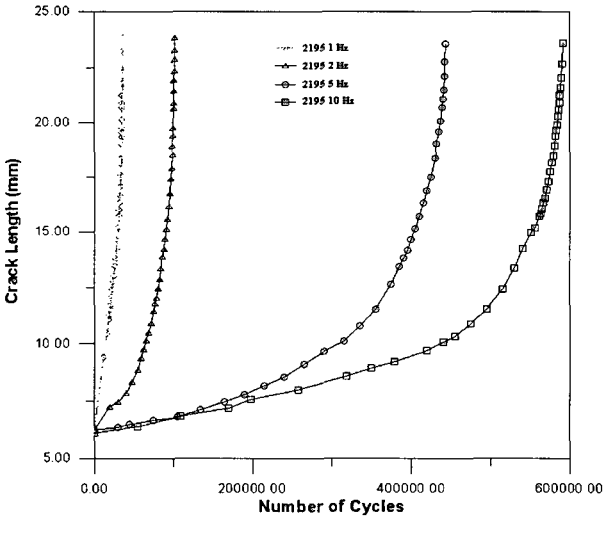

Figure 7: 2195 alloy

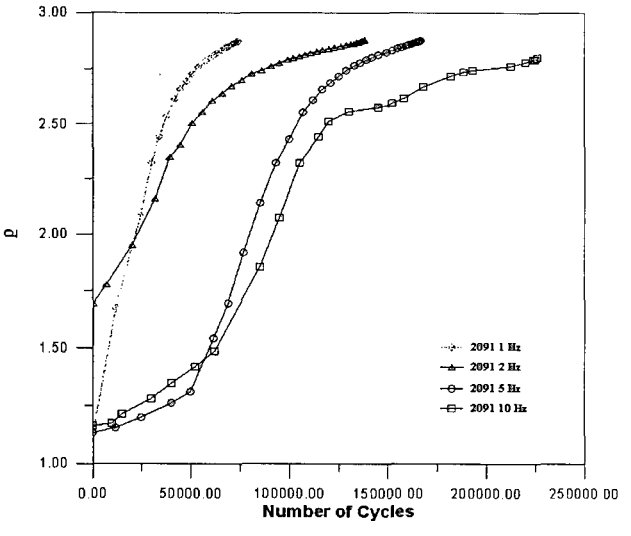

Figure 10: 2091 alloy

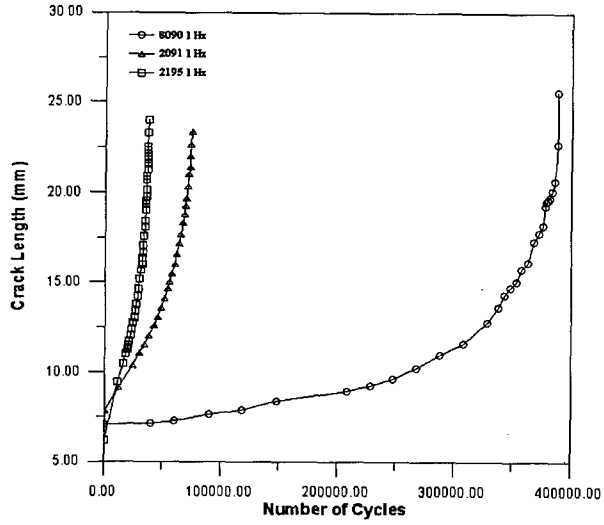

Figure 11: Comparison at 1 *Hz*

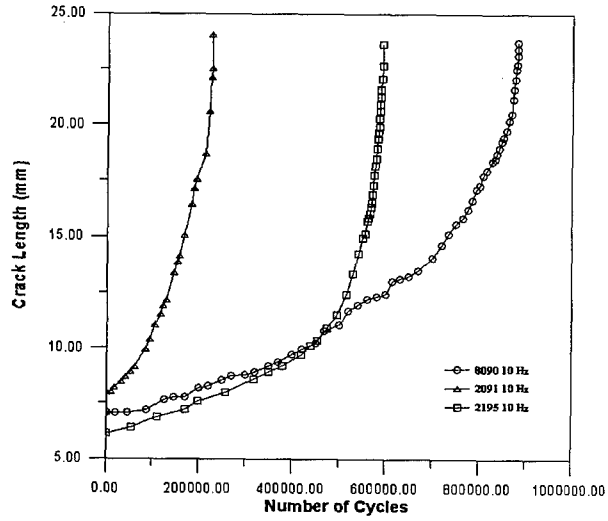

Figure 14: Comparison at 10 *Hz*

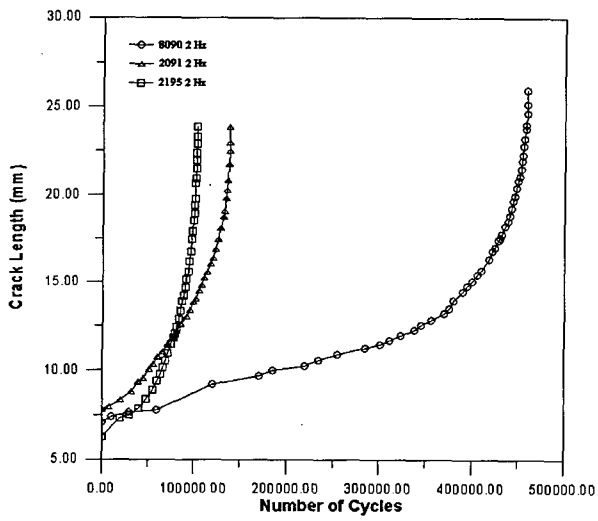

Figure 12: Comparison at 2 *Hz*

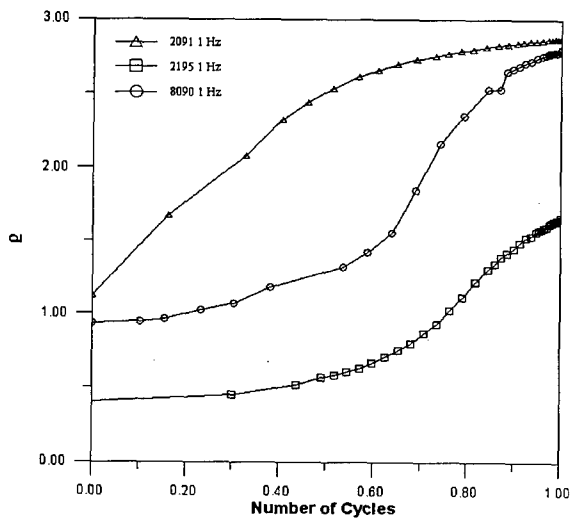

Figure 15: Comparison at 1 *Hz*

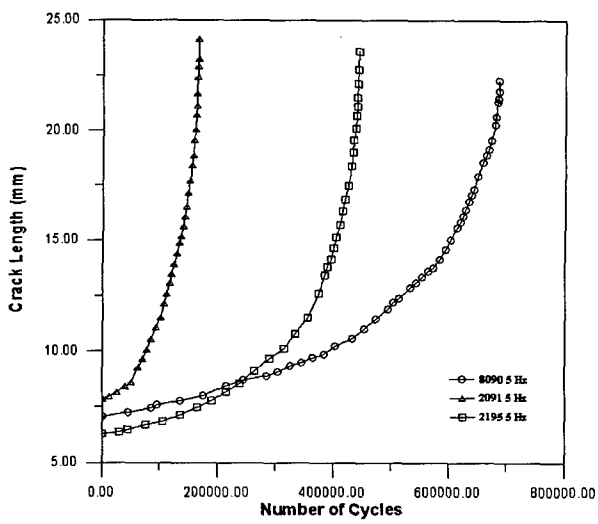

Figure 13: Comparison at 5 *Hz*

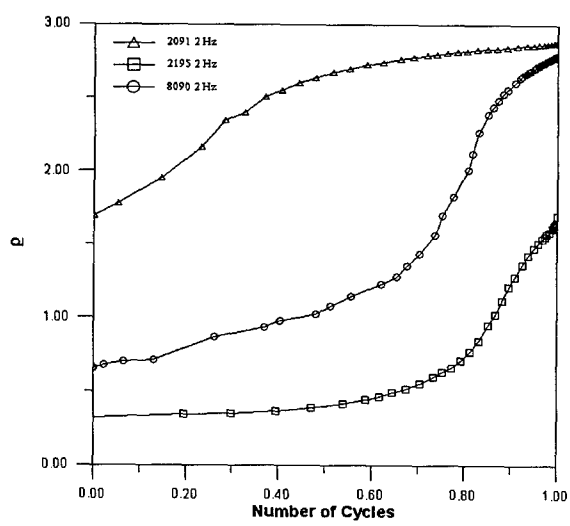

Figure 16: Comparison at 2 *Hz*

of plastic zone size. For such alloy, however, the gap between the curves at low frequency (1-2 Hz) and the curves at higher frequency (5-10 Hz) results comparably high, denoting a remarkable frequency effect even if a larger ammount of tests at lower and higher frequencies should still be provided. Finally the tests performed for the 2091 alloy are reported in Figg. 9-10. Similar results are obtained even if this alloy introduces more regular variation between frequencies.
In Figg. 11-12-13-14 are represented some comparative diagrams between the considered alloys. In order to facilitate a correct comparison, the curves are reported with frequency as parameter. Fatigue life for 8090 alloy is greater at any frequency, resulting much more evident at lower frequency.
In Figg. 15-16-17-18 plastic zone size (ρ) is plotted as function of the adimensional cycles number (n/N). In this case 2195 alloy, which shows better mechanical performances (in terms of yield and ultimate stress), seems to be less sensitive to the phenomenon of plasticity, always present at crack tip. In this context, 2091 alloy shows an extreme sensibility to plasticity, denoting, expecially at higher frequency, the largest plastic zone size. 8090 alloy assumes an intermediary role between the previous two (apart of the test at 10 Hz for n/N>0.8) showing a rather regular trend.
Wake plastic zone progress, which represents residual stress distribution on crack surfaces, is analysed through the monitoring of the first element length vs crack propagation. Generally its exponential behaviour has been found to change passing from 1 to 10 Hz, meaning that wake plastic zone is not only spreading on crack surfaces but also varying its shape. For the 2195 alloy, on the contrary, the exponential fitting curve (Fig. 19) remains a Vapor Pressure one, having a standard error close to 1 10^{-5} and a correlation coefficient of 0.999.

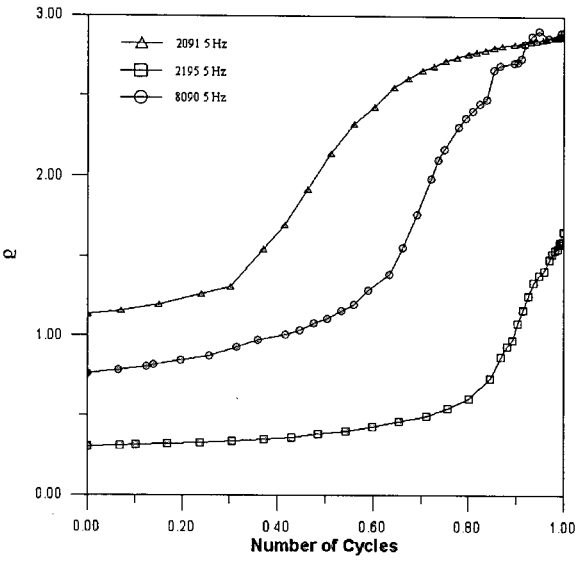

Figure 17: Comparison at 5 Hz

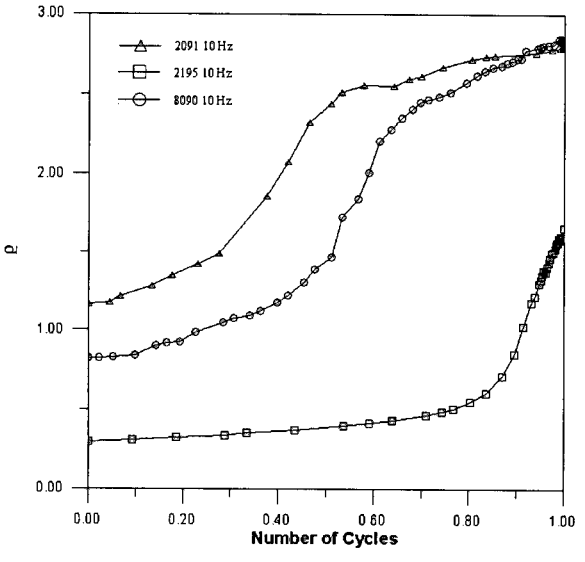

Figure 18: Comparison at 10 Hz

5. CRACK SURFACE ANALYSES

At the end of fatigue tests, specimen fracture surfaces have been analysed by SEM in order to individualise the characteristics of fracture as function of the frequency and ΔK.
The fatigue fracture of 8090 alloy could be investigated through two different models: Shear Facet Mode and Flat Tensile Mode. These depend obviously on the load conditions (R, S_{max}) and are influenced also by crack length and frequency. The Tensile Mode appeared dominant at low frequency and in regime of Short Cracks, while the Shear Mode did likewise at high frequency and in the regime of Long Cracks (Fig. 20). The transition from one mode to another depends upon crack lenght and applied load: this may lead to the definition of a variable parameter of the stress state as, for instance, K_{max}, ΔK or ΔK_{eff}. In fact, beyond an opportune critical value of ΔK_{eff}, fracture due to Tensile Mode is no longer present, while at lower values some mixed

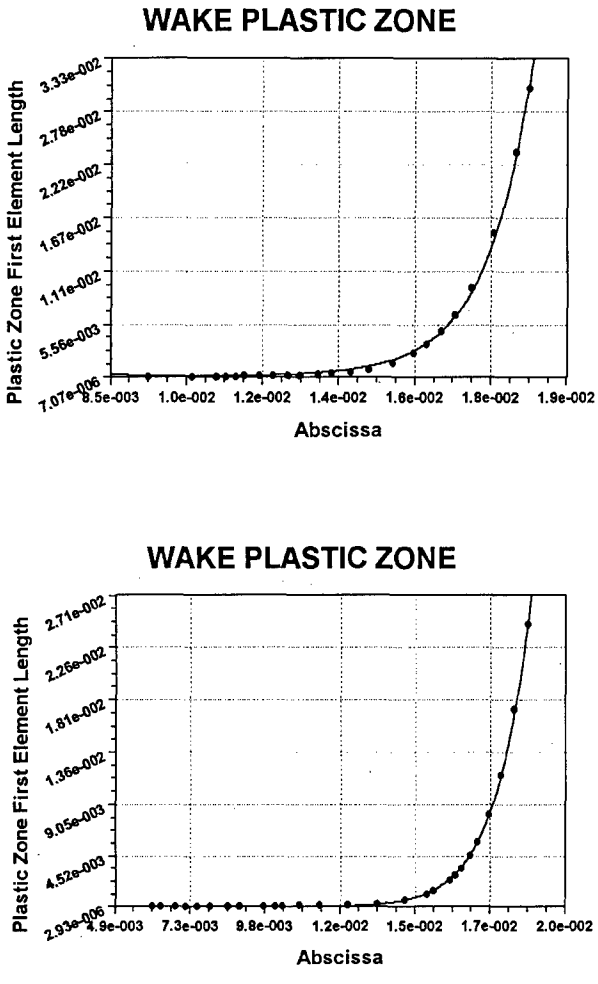

Figure 19: Wake plastic zone spreading for 2195 alloy

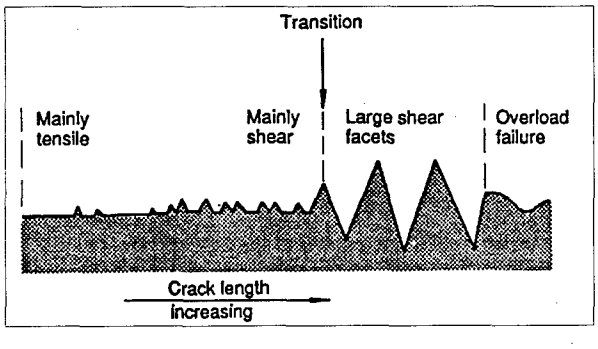

Figure 20: Fracture profile for 8090 alloy

ways of fracture may be observed (Shear + Tensile). Such marked dependence from the effective value of stress intensity factor, has been justified correlating the real dimension of the plastic zone (ρ) with the limit of diffusion of hydrogen per cycle. In other words, when ρ overcomes the distance of diffusion of hydrogen, a fracture is had preferentially by Shear type rather than Tensile type. Basing on this concept, for low values of the ΔK at 1 Hz (Photo 1), the surface shows mixed-mode fracture (Shear + Tensile), that tends, for higher values of the ΔK (Photo 2), to a Shear Mode fracture with the presence of delamination. Applying the chemical solution previously described, the fracture surface revealed (Photo 3) pits which denoted that the crystallografics planes of fracture are (100) type. At higher frequencies (Photo 4), fracture mode is primarily Shear Mode, with an accented roughness of the surface and therefore a notable effect of crack closure. The analysis, performed by Scanning Electron Microscope, for 2195 alloy has denoted the presence of overload and delamination. For instance, Photo 5 refers to the zone of threshold in the test at 5 Hz in which the overloads are well recognised. In the same test, fracture surface, at higher ΔK values, shows zones (along the whole specimen) with fatigue striatures (Photo 6, Photo 7). At collapse, the specimens show a ductile structure with dimples (cone and cup). Delamination occurs similarly to 2091 alloy (Photo 8). In the case of 2 Hz tests, 2195 alloy introduces, at threshold, a behaviour analogous to that at 5 Hz, with less evident overload. Furthermore at 4-8 $mm.$ distance from the threshold the fracture is similar to that of 5 Hz test while, at around 10 $mm.$ distance from the threshold, some fatigue striatures, less marked than in the test at higher frequency, appeared. At higher values of ΔK, just before collapse, is noticed the presence of "Aluminum Plaques" (Photo 9).

Finally in the Photos 10-11-12, at high values of the ΔK, it is easily noticeable, for 2091 alloy, a marked delamination. In this alloy, the surface treatment attack has been performed for the 5 Hz test: the evidence of fracture planes (100) has been much easier in proximity of collapse.

In 2195 alloy, the attack has been performed for the test at 5 Hz. In proximity of the threshold, fracture planes of (111) type have been individuated (Photo 13) while, as crack growth rate and ΔK increase, fracture planes of (110) type are observed (Photo 14).

Photo 1: 8090. Fracture surface

Photo 2: 8090. Delamination

Photo 3: 8090. Pits

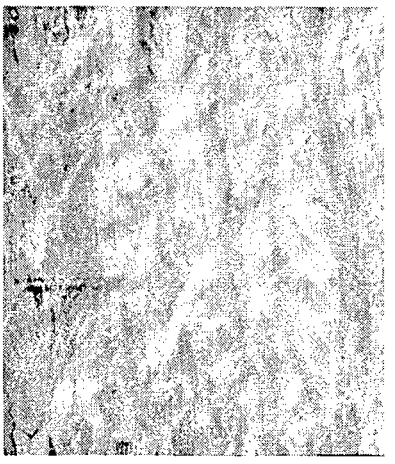

Photo 4: 8090. Roughness and crack closure

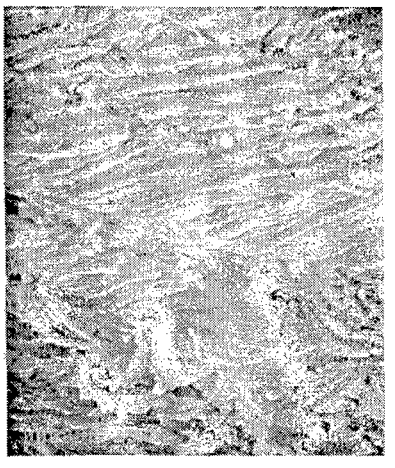

Photo 5: 2195. Overloads

Photo 6: 2195. Fatigue striatures

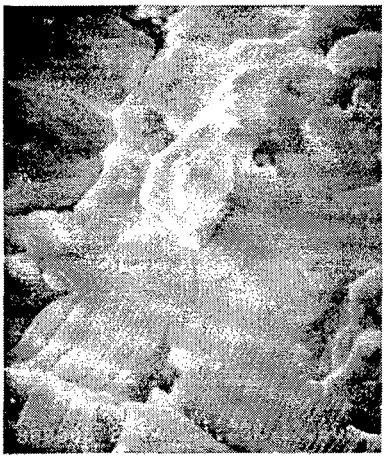

Photo 7: 2195. Fatigue striatures

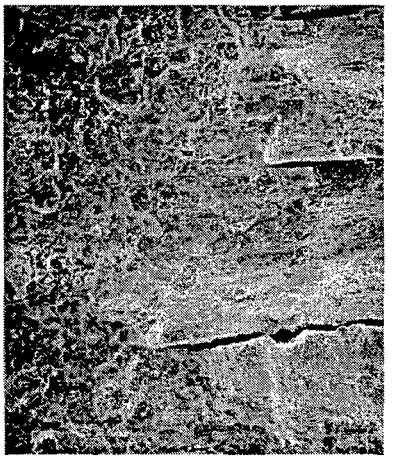

Photo 10: 2091. Delamination

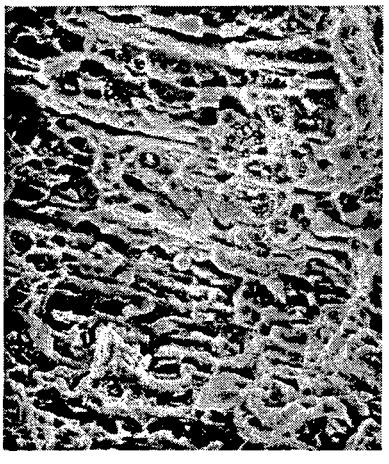

Photo 8: 2195. Delamination

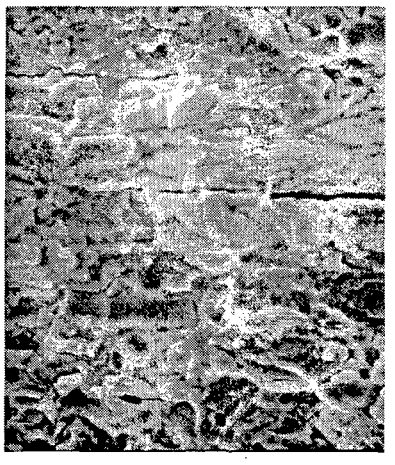

Photo 11: 2091. Delamination

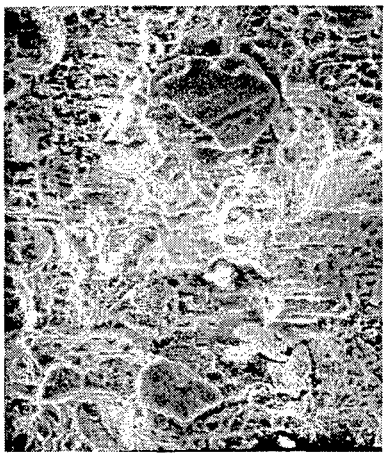

Photo 9: 2195. Aluminium Plaques

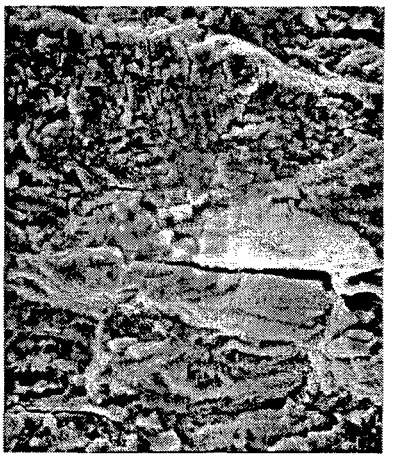

Photo 12: 2091. Delamination

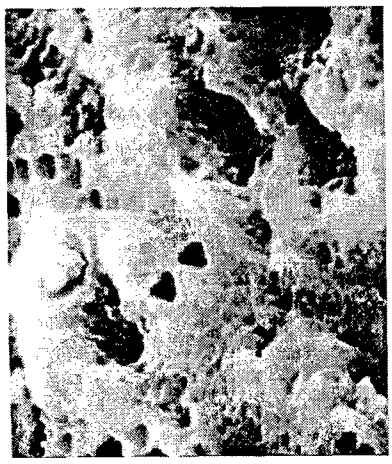

Photo 13: 2195. Fracture planes (111)

Photo 14: 2091. Fracture planes (110)

6. CONCLUSIONS

Fatigue tests on 2091, 2195 and 8090 Al-Li alloys have shown different behaviours in terms of ΔK_{th}, of maximum number of cycles and of plastic crack wake. Average values of ΔK_{th} pass from 3.45 $MPa\sqrt{m}$ for 2091 alloy to 4.40 and 4.58 respectively for 8090 and 2195 alloys, however imposing negligible crack growth for ΔK less then 15 $MPa\sqrt{m}$. While 8090 alloy showed the highest fatigue life at constant frequency in the range 1-10 Hz, 2195 alloy appeared particularly sensible at its variation denoting, as frequency effect, a large gap passing from 1-2 Hz to 5-10 Hz curves. 2195 alloy presented, also, the smallest ammount of plasticity at crack tip, while 2091 alloy showed the widest spreading. Plastic wakes, increasing in size exponentially as crack propagates, appeared to maintain their shape just for the case of 2195 alloy.
SEM crack surface analysis results can be summarized as follows:

- **8090**. Fracture planes of (100) type, evidence of delamination expecially close to failure, no clear striatures and strong effect of crack closure.
- **2195**. Fracture planes of (111) type and of (110) type respectively for low (close to threshold) and high ΔK, strong evidence of delamination close to failure and of fatigue striatures.
- **2091**. Fracture planes of (100) type not easily identificated at low ΔK but subsequently (at failure) much clearer, evidence of delamination and strong oxidation at each test frequency.

References

1. Ekvall J.C., Rhodes J.E., Wald G.C., Methodology for evaluating weights savings from basic material properties, Design of Fatigue and Fracture Resistant Structures, ASTM STP 761, Philadelphia, PA, USA, 1982, pp. 328-341.
2. Pell C.J., Evans B., Baker C.A., Bennet D.A., Gregson P.J., Flower H.M., The development and application of improved aluminium-lithium alloys, Aluminium-Lithium Alloys II, The Metallurgical Society of AIME, Warrendale, PA, USA, 1984, pp. 363-392.
3. Doker H., Bachmann V., Castro D.E., Marci G., Schwellwert fur Ermudungsribausbreitung: Ekvall Bestimmungsmethoden, Kennwerte, Einflubgroben, Z. Werkstofftech, 1987, 18, pp. 323-29.
4. Heaton M.D., On the calculation of Stress Intensity Factor Due to Thermal and Residual Stress Field, CEGB Research Report NW/SSD/RR/158/76, 1976.
5. Newman J.C., Edwards P.R., Short-crack growth behaviour in an aluminium alloy, an AGARD cooperative test programme, AGARD report No. 732, Advisory Group for Aerospace Research and Development, Neuilly-sur-Seine, France, December 1988
6. Parker A.P., Residual Stress Effect in Fatigue, ASTM STP 776, American Society for Testing and Material, 1982, pp. 13-31
7. Elber W., Damage Tolerance in Aircraft Structures, ASTM STP 486, American Society for Testing and Materials, 1971, pp. 230-242

Paper 12

Question by D. Chaumette

The paper did not present on one side analytical methods and on the other side experimental results. Was there a correlation between the two approaches. How was the plastic zone measurement done. What are the effects of plane stress - plane strain.

Author's reply

Experimental tests followed the crack length "a" from which (together with other parameters as W, L, R) the analytical model is able to calculate extension and shape of plastic zone through the use of a series of rigid elements (strip model). This model considers residual plastic deformation along crack surfaces and plastic zone ahead of crack tip.

Small fatigue cracks mostly induce plane-strain conditions. As plastic zone spreads out we assist at a transition to plane-stress conditions. This model, according to Newman, may pass, through the use of a correction factor ß (1-3) from one condition to another depending upon crack size. (5)